International Journal of Engineering Research
Volume No.4, Issue No.3, pp : 145 – 150
ISSN:2319-6890)(online),2347-5013(print)
01 March. 2015

A Stand Alone Robust PV-FC-Eletrolyzer Utilization Scheme

[1]Maged N. F. Nashed Mona Eskander, [2] Adel M Sharaf,Life
[1]Electronics Research Institute,Cairo, Egypt
[2] Senior Member IEEE,Sharaf Energy Systems, Inc., Fredericton, NB- Canada
maged@eri.sci.eg, Profdramsharaf@yahoo.ca

Abstract:*A stand-alone efficient robust photovoltaic (PV)-Electrolyzer Scheme using a PV-Array, a DC-DC buck-boost converter, an Electrolyzer, a hydrogen tank, and an additional Fuel Cell (FC) stack feeding an standalone autonomous load is investigated and validated for efficient energy utilization, voltage stabilization and maximum power point tracking (MPPT) of the PV array under different insolation and temperature variations. The DC-DC Converter by controlled to ensure stable regulated operation. The PV generated power is used to electrolyze water to Hydrogen H_2 and Oxygen O_2, where hydrogen is stored in a suitably sized tank to be used later for the PEM-Proton Exchange membrane fuel cell (PEMFC). The PEMFC also acts as supplementary energy storage and load balancer to supply dynamic variable load whose value can vary from a minimum of 300W to a maximum of 1Kw. The Hydrogen H_2 flow to the FC depends on the dynamic load variations. The controller is fully regulated for efficient energy utilization as well as voltage regulation. The validated scheme components are modeled using Matlab/Simulink and fully integrated, to assess the unified system dynamic performance under varying conditions.*

Keywords— PV, Buck-Boost converter, Electrolyzer, and PEMFC.

I. Introduction

The ever-increasing demand for with depleted resources and massive energy consumption in developing countries created a dilemma of rising cost and limited supplies with soaring fossil fuel cost and global environment impact. This created and accelerated increased interest in renewable and alternative green enery/power generation systems. Photovoltaic (PV) power generation is the most promising renewable power generation technologies. The growth of PV power generation systems has exceeded the most optimistic estimation [1-2]. A significant problem for renewable energy generation system is need for energy storage for supplying the load demand during absence of Sun. Energy storage can be done via batteries such as Cr-Fe, Cd-Ni, lead-acid and vanadium redox flow batteries (VRB), [3-4]. The VRB is a promising green solution in practical applications [5], due to the advantages of large scale, simple structure, long life cycle and high SOC. After many technological advances, proton exchange membrane FC technology has now reached the test and demonstration phase. FC also shows great potential as a green power source, in the future because of many merits they have such as high efficiency, zero or low emission of pollutant gases, flexible modular structure and the rapid progress in FC technologies. However, each of the aforementioned technologies has its own drawbacks. For instance, wind and solar power are highly dependent on climate while FC needs hydrogen-rich fuel. Nevertheless, different alternative energy sources can complement each other to some extent. Multisource hybrid alternative energy systems (with proper control) have great potential to provide higher quality and more reliable power to customers than a system based on a single resource, [6].

The dynamic nonlinear Voltage-versus-Current (V-vs-I) characteristic of a PV array, there is a unique maximum power point (MPP) at which the PV operates at its maximum output power. However, the MPP moves under different atmospheric conditions because of the output voltage and current of a PV array vary as the radiation and temperature change. Operating the PV array at its maximum available power increases its efficiency resulting in a decrease in the operating costs. Since, PV arrays are still considered rather expensive compared with the utility fossil fuel generated electricity costs. The PV system owner desires to get maximum power from the PV array and to operate it at its highest conversion efficiency, [7]. In this paper control and management a system composed of a PV array, buck-boost converter, an electrolyzer, a H_2 tank, a proton **e**xchange membrane fuel cell (PEMFC), and a 1Kw variable load is done. Each system component is modeled and integrated to demonstrate the system performance at different Insolation levels and load demand. A dynamic controller is designed and validated for Efficient Energy Utilization, Voltage Stabilization as well as load demand management.

II. System Modeling

1. PV Array Analysis

The solar cell equivalent circuit is demonstrated by Fig. 1. The model (V-vs-I) characteristic equation describing the PV cell operation is given as, [8]:

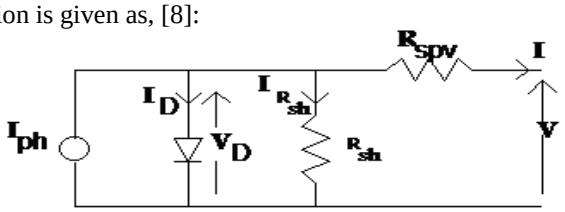

Fig. 1, PV- Cell Equivalent Circuit.

Assuming: 1- The temperature is constant at 300^{o} K (i.e. 27^{o} C).

2- The shunt resistance is too high, and consequently I_{sh} is neglected.

$$I_D = I_O\{\exp[A_{PV}(V + IR_{SPV})] - 1\} \quad (1)$$

where $A_{pv} = \frac{qV}{AKT}$

q: electron charge
K: Boltzmann's constant
A: completion factor

Numerical methods have been used to calculate the cell parameters by using the experimental data at three different points on the I-V characteristics, namely, the short circuit current (0, I_{SC}), the open circuit voltage (V_{OC},0) and the MPP

ISSN:2319-6890)(online),2347-5013(print)
01 March. 2015

(V_p, I_p). Also dynamic resistances $R_{so}= -(\frac{\partial V}{\partial I})_{V=V_{oc}}$ and $R_{shsc} =-(\frac{\partial V}{\partial I})_{I=I_{sc}}$ are obtained at the respective points. The equation of the generated current, which consists of N_s cells in series and N_p cells in parallel, is given by:

$$I_{pv} = I_{phg} - I_{og}\{\exp[A_g(V_{pv} + I_{pv}R_{sg})] - 1\} - \frac{V_{pv} + I_{pv}R_{sg}}{R_{shg}} \quad (2)$$

The model of PV array in Matlab/Simulink software is shown in Fig. 2. The voltage-current characteristic curves of PV model under different irradiances are given in Fig. 3.

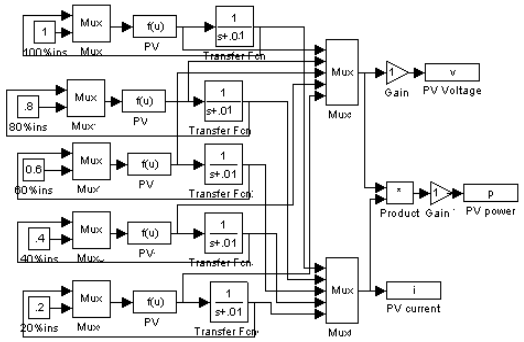

Fig. 2, PV array Matlab/Simulink model for varying Insolation

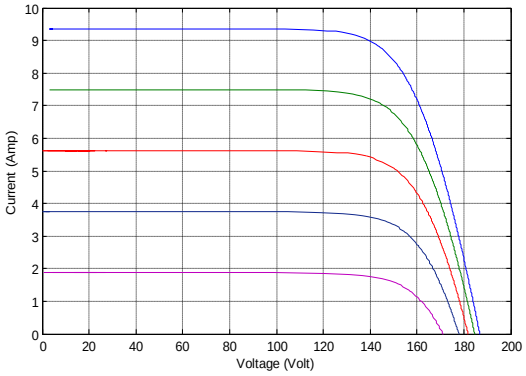

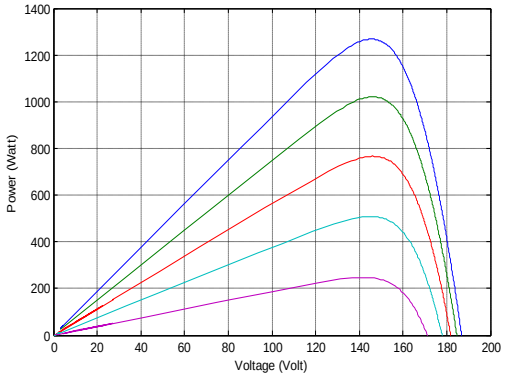

Fig.3, V-I-P Relations between voltage, current and power of the PV array at different Insolation.

The voltage at MPP is used as a reference value in the controllers in order to be tracked. The relation between the voltage at MPP and Insolation (ϕ) can be expressed as a second order polynomial given by:

$$V_{ref} = V_P = -0.0018\phi^2 + 0.2709\phi + 136.4725 \quad (3)$$

This relation is shown in Fig. 4

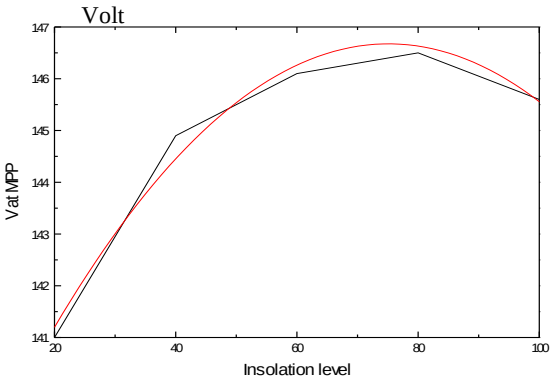

Fig. 4, V-vs-φ Relation between voltage at MPP and Insolation level φ.

2. DC-DC Converter-Buck-Boost

An ideal Buck-Boost converter is used to interface the PV array source to the electrolyzer Load Cell. With the assumption of ideal circuit elements, two switched models are shown in Fig. 5. State variables for this Buck-Boost converter are chosen as the inductor current, $I_L \equiv X_1$, and the capacitor voltage, $V_c \equiv X_2$. State-space-averaged equations in matrix form are, [11]:

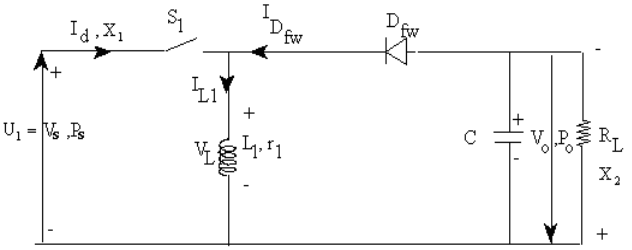

Fig. 5, Switched models for the ideal Buck-Boost converter.

$$\begin{bmatrix} \dot{X}_1 \\ \dot{X}_2 \end{bmatrix} = \begin{bmatrix} 0 & \frac{(1-D)}{L} \\ -\frac{(1-D)}{C} & -\frac{1}{RC} \end{bmatrix} \begin{bmatrix} X_1 \\ X_2 \end{bmatrix} + \begin{bmatrix} \frac{D}{L} \\ 0 \end{bmatrix} [U_1] \quad (4)$$

3. Electrolyzer

The Electrolyzer is a device that produces hydrogen and oxygen from water. Water-Eelectrolysis can be considered as a reverse process of a hydrogen PEM- fuel cell. The electrolyzer converts the DC electrical energy into chemical energy stored in hydrogen. Currently, there are three principal types of electrolyzer available in the market: alkaline, PEM, and solid oxide, [12].

The alkaline and PEM-Electrolyzers are well established devices with thousands of units in operation, while the solid-oxide Electrolyzer is as yet unproven [13]. Alkaline water electrolysis is the dominating technology today. In this section, the principle of alkaline water electrolysis is reviewed. An alkaline Electrolyzer uses potassium hydroxide (KOH) as electrolyte solution for transferring hydroxyl ions. Fig. 6 shows the schematic diagram of an alkaline Electrolyzer.

At the cathode, two water molecules are reduced electrochemically (by the two electrons from the cathode) to one molecule of H2 and two hydroxyl ions (OH^-). The reaction at the cathode can be expressed as:

ISSN:2319-6890)(online),2347-5013(print)
01 March. 2015

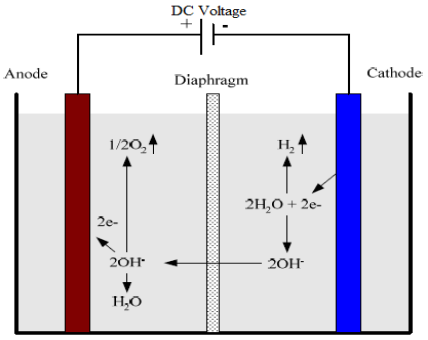

Fig. 6, Schematic diagram of an alkaline type Electrolyzer.

$$2H_2O + 2e^- \Rightarrow H_2 \uparrow + 2OH^- \quad (5)$$

Under the external electric field, the hydroxyl ions are forced to move towards the anode through the porous diaphragm. At the anode, the two molecule hydroxyl ions, losing two electrons to the anode, are discharged into 1/2 molecule of O_2 and one molecule of water. The chemical reaction at the cathode is

$$2OH^- \Rightarrow \tfrac{1}{2} O_2 \uparrow + H_2O + 2e^- \quad (6)$$

By combining the above two equations, the overall chemical reaction inside an electrolyzer is

$$2H_2O \Rightarrow H_2 \uparrow + \tfrac{1}{2} O_2 \uparrow \quad (7)$$

The current density of alkaline-Electrolyzers is normally less than 0.4 A/cm^2. The energy conversion efficiencies can range from 60-90%. Without auxiliary purification equipment, purities of 99.8% for H_2 can be achieved. Alkaline electrolysis technology can be implemented at a variety of scales from less than 1 kW to large industrial electrolyzer plant over 100 MW as long as there is a proper DC electricity supply [14]. The model of an electrolyzer stack developed for this study is based on the empirical *I–V* equation reported in [15], described as

$$V_{elec,cell} = V_{rev} + \frac{r_1 + r_2 T}{A} I + k_{elec} \ln\left(\frac{k_{T1} + k_{T2}/T + k_{T3}/T^2}{A} I + 1\right) \quad (8)$$

where *V*elec,cell is the cell terminal voltage (in volts),
*V*rev is the reversible cell voltage,
r_1 (in ohms square-meter) and *r*2 (in ohms square-meter per degree Celsius) are the parameters for the ohmic resistance inside the electrolyzer,
k_{elec} (in volts), k_{T1} (in square meters per ampere), k_{T2} (square-meter degrees Celsius per ampere), and k_{T3} (square-meter degree Celsius square per ampere) are the parameters for the overvoltage,
A is the area of the cell electrode (in square-meters),
I is the electrolyzer current (in amperes),
and *T* is the cell temperature (in degrees Celsius).

The *V–I* characteristics of the electrolyzer model used in this study at different cell temperatures are given in Fig. 7. At a given current, the higher the operating temperature, the lower is the terminal voltage needed.

According to Faraday's law, hydrogen production rate for an Electrolyzer cell is directly proportional to the electrical current in the equivalent Electrolyzer circuit [16].

$$n_{H_2} = \frac{\eta_F n_c i_e}{2F} \quad (9)$$

where i_e is the electrolyzer current,
n_c is the number of electrolyzer cells in series,
and η_F is the Faraday efficiency.

Assuming that the working temperature of the electrolyzer is 40 ℃, Faraday efficiency is expressed by [8]

$$\eta_F = 96.5e^{(0.09/i_e - 75.5/i_e^2)} \quad (10)$$

Using equations (9) and (10), a simple electrolyzer model is developed using Simulink.

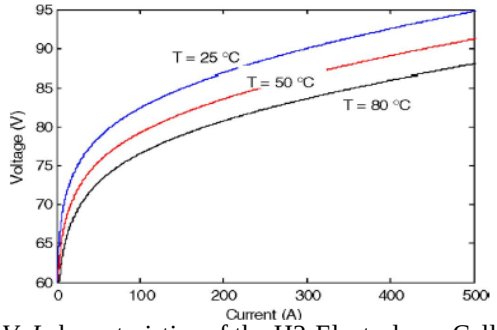

Fig. 7, *V–I* characteristics of the H2-Electrolyzer Cell model under different temperatures.

4. Hydrogen Storage Tank (HST) Modeling

Physical hydrogen storage is one of the storage techniques that use tank to store compressed hydrogen. The model of HST is described according to equation (11), [17] and using the ratio of hydrogen flow to the tank, directly obtained the tank pressure.

$$P_b - P_{bi} = z((n_{H_2} - W_{H_2})RT_b / M_{H_2} V_b) \quad (11)$$

Where: R is universal gas constant [J (kmol $^oK)^{-1}$]
P_b is Pressure of tank [P_a]
P_{bi} is Initial pressure of the storage tank [P_a]
W_{H2} is hydrogen flow rate delivered to FC,
M_{H2} is hydrogen mass
T_b is Tank operating temperature [°K]
V_b is volume of the tank [m^3]
z is compressibility factor as a function of tank pressure

5. Proton Exchange Membrane Fuel Cell (PEMFC)

FC converts oxygen and hydrogen chemical energy to electrical energy. The amount of output voltage in each cell is small. Therefore, cells are connected in series to gain a higher output voltage. Three basic are as which affect the output voltage are ohmic, activation and concentration polarization [18]. FC output voltage is mentioned in polarization curve calculated by:

$$VFC = E_{nernst} - V_{act} - V_{ohmic} - V_{con} \quad (12)$$

The open circuit voltage in FC which is denoted by E_{nernst} can be defined as follows:

$$E_{nernst} = 1.229 - 0.85*10^{-3}(T - 298.15) + 4.3085*10^{-5} T[\ln(P_{H_2}) + 0.5\ln(P_{O_2})] \quad (13)$$

where:T is refers to FC operation temperature, [^oK];
P_{H2} & P_{O2} are partial pressure of hydrogen & oxygen, [atm].

Ohmic polarization shows ohmic voltage drop due to resistive losses in the cell which is caused by resistance against electrons and ions movement. The ohmic voltage drop can be defined as follows:

$$V_{ohmic} = i_{FC}(R_M + R_C) \quad (14)$$

where: i_{FC} is refers to FC current;
R_C is resistance of FC electrodes against electrons movement which is constant;

ISSN:2319-6890)(online),2347-5013(print)
01 March. 2015

R_M is FC membrane resistance against ions passing, which equal $\rho_M(l/A)$, [19].

Activation polarization shows activation voltage drops in FC anode and cathode electrodes. These drops are caused by the slow reactions on the surface of electrodes which are calculated by:

$$V_{act} = -[\xi_1 + \xi_2 T + \xi_3 T \ln(C_{O_2}) + \xi_4 T \ln(i_{FC}) \quad (15)$$

where CO_2 is the oxygen concentration rate on the catalyst surface.

Concentration polarization shows voltage drop due to reduction in density of reaction materials which is called mass transport losses. To determine voltage drop model due to mass transport, maximum current density must be gained (J_{max}). Voltage drop corresponding to mass transport can be calculated by [20]:

$$V_{con} = -B\ln(1-(J/J_{max})) \quad (16)$$

Considering all FCs voltage drops and for n cells which are connected in series by forming a stack, output power of FC stack is defined as follows:

$$P_{FC} = N_{FC}\, V_{FC}\, I_{FC} \quad (17)$$

where N_{FC} represents the number of cells in series.

The FC current i_{FC} can be determined as a function of hydrogen flow rate to FC and can be obtained by [21]:

$$i_{FC} = (2F/N_{FC})(W_{H2}/M_{H2}) \quad (18)$$

where: W_{H2} is hydrogen molar flow rate delivered to FC, M_{H2} is hydrogen molar mass and F refers to Faraday's constant [C/kmol].

III. Power Management

An overall control strategy for power management among PV array with buck boost converter, electrolyzer and Hydrogen tanks PEMFC and variable load is designed. Fig. 8 shows the block diagram of the overall control strategy for the proposed system. PV electricity generation unit controlled for voltage regulation controller.

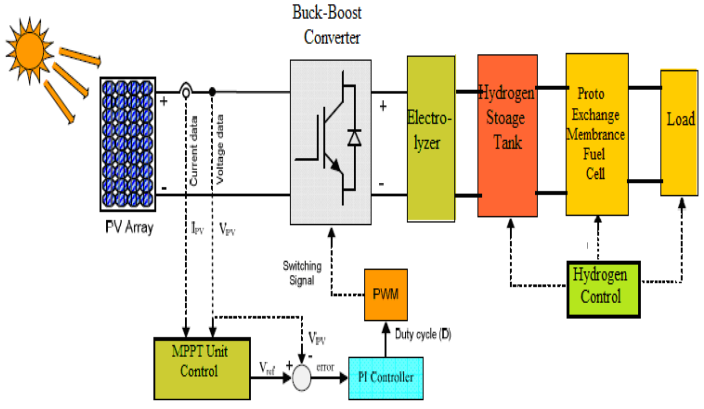

Fig. 8, Block diagram of the overall PV-FC-Electrolyzer Energy Scheme

IV. Digital Simulation Results and Discussion

System input data includes load electricity demand and solar radiation during 24 h. A load varying between 300W and 1kW along 24 hours is assumed. The demand of load electricity during 24 h is depicted in Fig. 9. The rates of hydrogen production by EL, consumed hydrogen by PEMFC and stored hydrogen in HST are shown in Fig. 10. Figures 9 and 10 demonstrate the hydrogen consumed by the distributed load during the night (from 12:00 AM till 6:30 AM). As the sun rises it is clear that the amount of stored hydrogen that is consumed by the load decreases, while the hydrogen level in the tank is increasing. This increase in hydrogen level continues until 5:00PM, after which as the insolation level decreases, the H_2 level in the tank starts decreasing while supplying the load demand. Fig. 11 shows the simulation system. Fig. 12 shows the insolation level with change from low to high at t=0.1 sec and change from high to low at t=0.15 sec. While, Fig. 13 shows the simulation results of voltage and current of photovoltaic at change in insolation level. It shows the controller performance as described in equation (3).

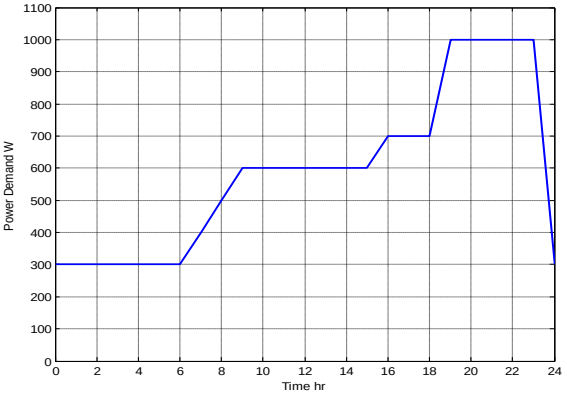

Fig. 9, 24 Hour-Load-Demand.

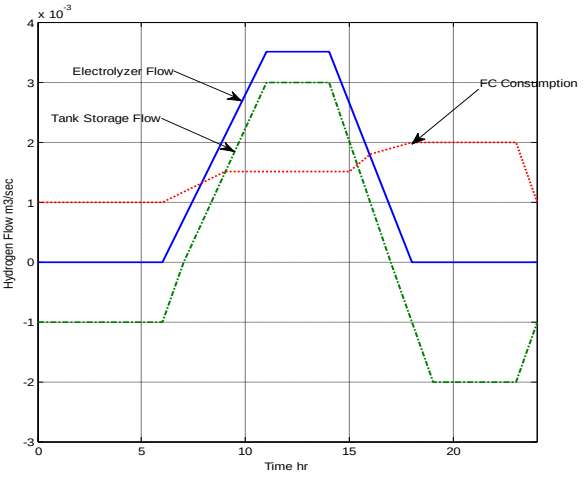

Fig 10, The Hydrogen flow

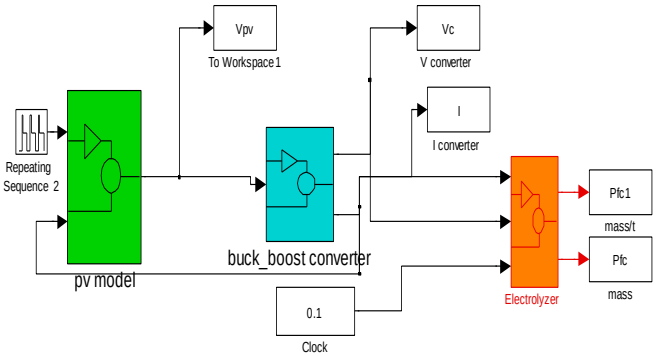

Fig. 11, Simulation of the system.

ISSN:2319-6890)(online),2347-5013(print)
01 March. 2015

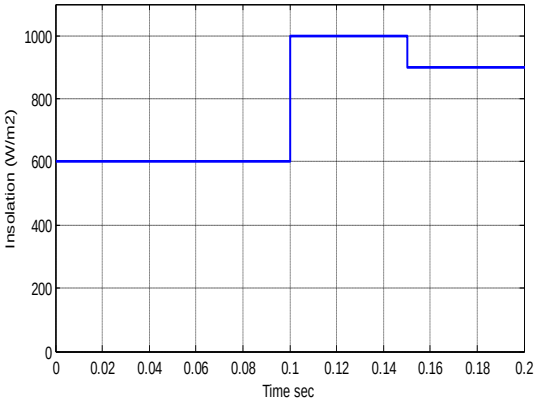

Fig. 12, Change of insolation.

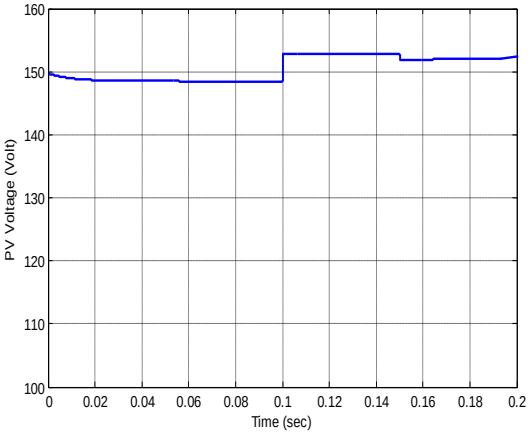

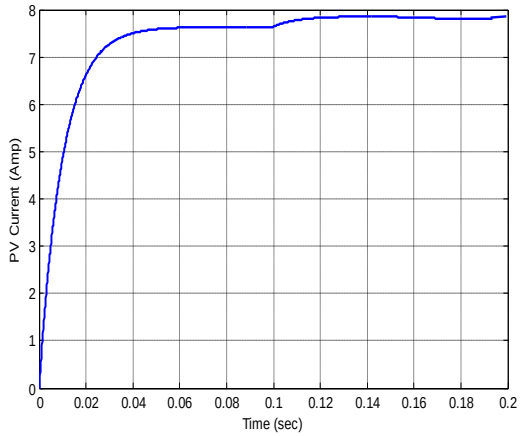

Fig. 13, the simulation results of Voltage and Current photovoltaic at change of insolation.

Fig. 14 shows the output voltage converter at MPP voltage and voltage regulator. It compares the converter output with MPP control, and when applying constant voltage control. The output voltage of the PV array is regulated at 145 V. This is because the variation of the output voltage, when following MPP, reaches 141V at a 20% Insolation level, and 146.5 at 80% Insolation level. Hence regulating the output voltage at the 146.5V outweighs its slight variation by 2.8|% only between the maximum and minimum Insolation level. Figures 15 and 16 show the converter supplying the Electrolyer, revealing the rate of hydrogen flow to be stored in the tank. These figures show the time required for filling the H_2 tank is about 4 hours.

IV. Conclusion

An efficient regulation and control system for Power/demand load regulation of the flow of power generated by PV array to supply a variable load demand is designed. To ensure continuous supply of load, storage system is designed. The H2-storage system consists of an Electrolyer, H_2 tank with PV source and Fuel Cell storage and backup energy fuel cell. Maximum power utilization using the PV-MPPT based voltage regulator is fully validated under varying condition. Unified System components are modeled, and dynamic simulation results validated the robustness and damping behaviour under varying insolation and load conditions. He proposed scheme can be extended to PV Farm Utilization and Village/Island/Village Electricity.

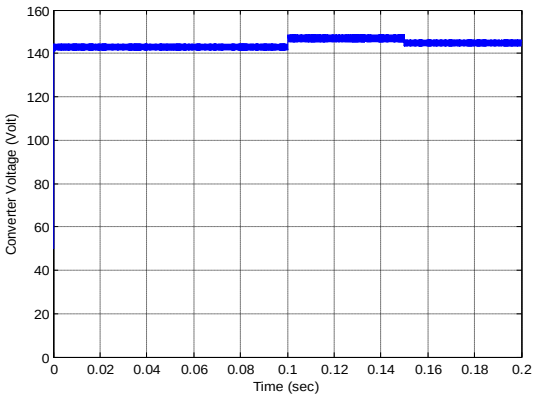

(a) MPP Voltage

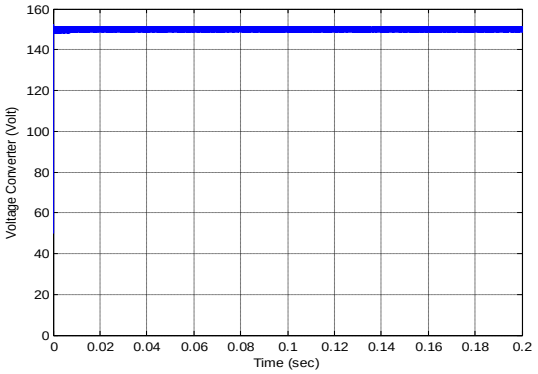

(b) Voltage Regulator

Fig. 14, Output voltage of Converter

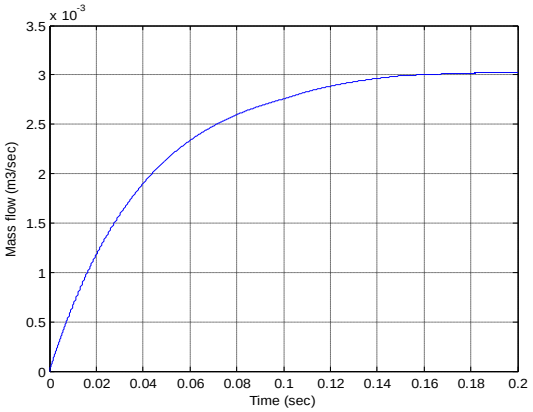

Fig. 15, Output of hydrogen flow from Electrolyer

ISSN:2319-6890)(online),2347-5013(print)
01 March. 2015

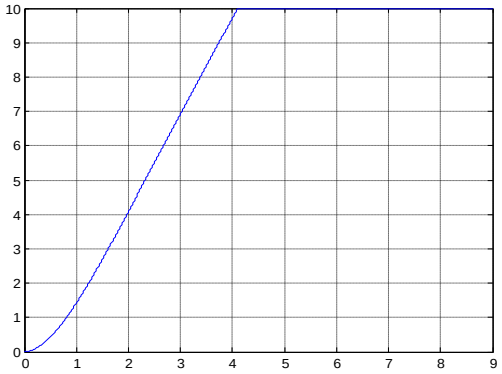

Fig. 16, the hydrogen storage tank

References

i. *Trends in Photovoltaic Applications: Survey Report of Selected IEA Countries between 1992 and 2004, International Energy Agency Photovoltaic Power Systems Programme (IEA PV, January 2005, pp: 1–22.*

ii. *Global Wind report, Global Wind Energy Council. http://www.gwec.net/index*

iii. *F. Chekired, C. Larbes, and A. Mellit, "Comparative study between two intelligent MPPT-controllers implemented on FPGA: application for photovoltaic systems" International Journal of Sustainable Energy, Vol. 33, No. 3, May 2014, pp: 483-499.*

iv. *R. Cakmak, I. H. Altas, and A. M. Sharaf "Modeling of FLC-Incremental Based MPPT using DC-DC Boost Converter for Standalone PV System" International Symposium on Innovations in Intelligent Systems and Applications (INISTA), 2-4 July 2012, Turkey*

v. *W. H. Wang and X. D. Wang, "Analysis and Measurement of SOC in the Vanadium Flow Battery," Journal of Zhejiang University of Technology, Vol. 34, Apr. 2006.*

vi. *K. Sapru, N. T. Stetson, and S. R. Ovshinsky, "Development of a small scale hydrogen production storage system for hydrogen applications," in Proc. the 32nd Intersociety Conference, vol. 3, pp. 1947-1952, 1997.*

vii. *I.H. Altas and A.M. Sharaf, "A novel maximum power fuzzy logic controller for photovoltaic solar energy systems", Renewable Energy, vol. 33, no.3, pp. 388-399, 2008.*

viii. *F. Harasima, H. Inaba, and N. Takashim, "Microprocessor-Controlled SIT Inverter for Solar Energy System", IEEE Transactions on Industrial Electronic, Vol. IE-34, No. 1, Feb. 1987, pp. 50-55.*

IX. *A. M. A. Mahmoud, H. M. Mashaly, S. A. Kandil, H. EL Khashab, and M. N. F. Nashed, "Fuzzy Logic Implementation for Photovoltaic Maximum Power Tracking", 6th International Conference on Soft Computing, IIZUKA 2000, Iizuka, Fukuoka, Japan, Oct. 1-4,2000, pp 732-737*

x. *B. Kumar, Y. K. Chauhan, and V. Shrivastava, "Performance analysis of a water pumping system supplied by a photovoltaic generator with different maximum power point tracking techniques" Songklanakarin Journal of Science and Technology, Vol. 36, No. 1, 2014, pp: 107-113.*

xi. *N. Mohan, T. M. Undrland, and W. P. Robbius, "Power Electronics: Converters, Applications and Design", 1995 by john Wiley and Sons, Inc.*

xii. *W. Kreuter and H. Hofmann, "Electrolysis: The Important Energy Transformer in a World of Sustainable Energy," Int. J. Hydrogen Energy, Vol. 23, No.8, 1998, pp. 661-666.*

xiii. *M. Newborough, "A Report on Electrolysers, Future Markets and the Prospects for ITM Power Ltd's Electrolyser Technology,", http:// www.h2fc.com/Newsletter/*

xiv. *A.F.G Smith and M. Newborough, "Low-Cost Polymer Electrolysers and Electrolyser Implementation Scenarios for Carbon Abatement," Report to the Carbon Trust and ITM-Power PLC, Nov. 2004.*

xv. *O. Ulleberg and S. O. Morner, "TRNSYS simulation models for solar hydrogen systems," Solar Energy, vol. 59, no. 4–6, pp. 271–279, 1997.*

xvi. *S. M. Shaahid and M. A. Elhadidy, "Technical and economic assessment of gidindependent hybrid photovoltaic-diesel-battery power systems for commercial loads in desert environments," Renewable and Sustainable Energy Reviews, pp. 1794-1810, Oct. 2007.*

xvii. *J.K. Kaldellis, D. Zafirakis, and E. Kondili "Optimum sizing of photovoltaic-energy storage systems for autonomous small islands" International Journal of Electrical Power & Energy Systems, Vol. 32, No. 1, January 2010, pp. 24-36.*

xviii. *W. Friede, S. Rael, and B. Davat, "Mathematical Model and Characterization of the Transient Behavior of a PEM Fuel Cell" IEEE Trans. Power Electronics, Vol. 19, No. 5, Sept 2004, pp: 1234–1241.*

xix. *Pathapati P., Xue X., Tang J., A New Dynamic Model for Predicting Transient Phenomena in a PEM Fuel Cell System. Renewable Energy, Vol. 30, No. 1Stand-Alone PEM Fuel Cell Power Plant for Residential Applications" Journal of Power Sources, Vol. 138, No. 1–2, Nov. 2004, pp: 199–204.*

xx. *P. Buasri, and Z. M. Salameh., "An Electrical Circuit Model for a Proton Exchange Membrane Fuel Cell (PEMFC)" IEEE Power Engineering Society General Meeting, 2006.*

xxi. *M. Y. El-Sharkh, A. Rahman, M. Y. Alam, P. C. Byrne, A. A. Sakla, and T. Thomas, "A Dynamic Model for a PS), Sep. 2005, www.iea-pvps.org*